

Negative-charge-storing mechanism of potassium-ion SiO₂-based electrets for vibration-powered generators

Cite as: Appl. Phys. Lett. **117**, 193902 (2020); <https://doi.org/10.1063/5.0029012>

Submitted: 09 September 2020 . Accepted: 01 November 2020 . Published Online: 10 November 2020

 Toru Nakanishi, Takeshi Miyajima, Kenta Chokawa,  Masaaki Araidai,  Hiroshi Toshiyoshi, Tatsuhiko Sugiyama, Gen Hashiguchi, Kenji Shiraishi, et al.



View Online



Export Citation



CrossMark

ARTICLES YOU MAY BE INTERESTED IN

[Charging mechanism of electret film made of potassium-ion-doped SiO₂](#)

AIP Advances **6**, 035004 (2016); <https://doi.org/10.1063/1.4943528>

[Pure spin current phenomena](#)

Applied Physics Letters **117**, 190501 (2020); <https://doi.org/10.1063/5.0032368>

[Slow propagation of 2 GHz acoustical waves in a suspended GaAs phononic waveguide on insulator](#)

Applied Physics Letters **117**, 193501 (2020); <https://doi.org/10.1063/5.0019949>

HIDEN
ANALYTICAL

Instruments for **Advanced Science**

- Knowledge,
- Experience,
- Expertise

[Click to view our product catalogue](#)

Contact Hiden Analytical for further details:

www.HidenAnalytical.com
info@hiden.co.uk



Gas Analysis

- ▶ dynamic measurement of reaction gas streams
- ▶ catalysis and thermal analysis
- ▶ molecular beam studies
- ▶ dissolved species probes
- ▶ fermentation, environmental and ecological studies



Surface Science

- ▶ UHVTPD
- ▶ SIMS
- ▶ end point detection in ion beam etch
- ▶ elemental imaging - surface mapping



Plasma Diagnostics

- ▶ plasma source characterization
- ▶ etch and deposition process reaction kinetic studies
- ▶ analysis of neutral and radical species



Vacuum Analysis

- ▶ partial pressure measurement and control of process gases
- ▶ reactive sputter process control
- ▶ vacuum diagnostics
- ▶ vacuum coating process monitoring

Negative-charge-storing mechanism of potassium-ion SiO₂-based electrets for vibration-powered generators

Cite as: Appl. Phys. Lett. **117**, 193902 (2020); doi: 10.1063/5.0029012

Submitted: 9 September 2020 · Accepted: 1 November 2020 ·

Published Online: 10 November 2020



View Online



Export Citation



CrossMark

Toru Nakanishi,^{1,a)} Takeshi Miyajima,¹ Kenta Chokawa,^{2,b)} Masaaki Araidai,^{1,2} Hiroshi Toshiyoshi,³ Tatsuhiko Sugiyama,⁴ Gen Hashiguchi,⁴ and Kenji Shiraishi^{1,2}

AFFILIATIONS

¹Graduate School of Engineering, Nagoya University, Nagoya 464-8603, Japan

²Institute of Materials and Systems for Sustainability, Nagoya University, Nagoya 464-8601, Japan

³Institute of Industrial Science, The University of Tokyo, 4-6-1 Komaba, Meguro-ku, Tokyo 153-8505, Japan

⁴Research Institute of Electronics, Shizuoka University, 3-5-1 Johoku, Naka-ku, Hamamatsu, Shizuoka 432-8011, Japan

^{a)}Electronic mail: nakanishi.toru@e.mbox.nagoya-u.ac.jp

^{b)}Author to whom correspondence should be addressed: chokawa@fluid.cse.nagoya-u.ac.jp

ABSTRACT

A potassium-ion electret, which is a key element of vibration-powered microelectromechanical generators, can store negative charge almost permanently. However, the mechanism by which this negative charge is stored is still unclear. We theoretically study the atomic and electronic structures of amorphous silica (a-SiO₂) with and without potassium atoms using first-principles molecular-dynamics calculations. Our calculations show that a fivefold-coordinated Si atom with five Si–O bonds (an SiO₅ structure) is the characteristic local structure of a-SiO₂ with potassium atoms, which becomes negatively charged and remains so even after removal of the potassium atoms. These results indicate that this SiO₅ structure is the physical origin of the robust negative charge observed in potassium-ion electrets. We also find that the SiO₅ structure has a Raman peak at 1000 cm⁻¹.

Published under license by AIP Publishing. <https://doi.org/10.1063/5.0029012>

Energy-harvesting technology, which converts energy in the environment from sources such as light, heat, and vibration into electrical power, is a key element in meeting energy demands.^{1–4} Many types of energy-harvesting devices have been proposed, and these include thermoelectric devices and vibration-powered generators. Such devices tend to have maximum power outputs of several μW to a few mW, and they, therefore, have had limited conventional uses. However, in recent years, the range of applications for energy-harvesting devices has expanded due to the development of low-power technology. In particular, maintenance-free autonomous power supplies are very important for the Internet of Things and the Trillion Sensors⁵ initiative. Energy-harvesting technology has, therefore, attracted a significant amount of attention in relation to these technologies.

Among the many energy-harvesting technologies, vibration-powered generation is expected to provide a stable supply of electricity because its output does not depend on specific energy sources in the natural environment such as sunlight. Accordingly, vibration-powered generators can be widely used as stand-alone power sources for

sensors in environments with vibration, such as transportation machinery, roads, and wearable devices.⁶ Recently, a vibration-powered microelectromechanical generator with a potassium-ion electret has attracted increasing attention.^{7–12}

The factor that contributes to the power output in vibration-powered generation is described by the change in capacitance. It is possible to create narrow gaps by using a potassium-ion electret and to produce large changes in the electrical capacitance, thus increasing the power output. This is referred to as vibrational acceleration. In addition, the lifetime of a potassium-ion electret has been estimated to be about 400 years by accelerated tests.¹³ Therefore, a potassium-ion electret is superior to other electret materials.

A potassium-ion electret can be fabricated by adding potassium atoms to amorphous silica (a-SiO₂) and then subsequently removing them. A potassium-ion electret can permanently store a negative charge, and this enables the creation of maintenance-free power-generation devices. However, the mechanism by which this negative charge is stored in potassium-ion electrets is still unclear. In general,

the Si atoms in a-SiO₂ form four Si–O bonds, resulting in a fourfold coordinated structure having no characteristic defects with negative charges. Hence, it is important to clarify the role of potassium atoms in forming negatively charged defects in a-SiO₂.

With regard to potassium-incorporated SiO₂, K₂O–SiO₂ glasses have been intensively studied.^{14–19} In these materials, the K₂O densities are around 10%–50%. In a potassium-ion electret, however, the potassium density is about 0.01% (10¹⁹ cm⁻³)⁷ so that the potassium atoms have to be considered as impurity atoms. Thus, a system based on a potassium-ion electret is very different from conventional K₂O–SiO₂ glasses.

In this study, we simulated the manufacturing processes of potassium-ion electrets using first-principles calculations and created a-SiO₂ structures containing potassium atoms. We were then able to reveal the characteristic local structures formed by the presence of potassium atoms, and we examined the charge state in a local structure to clarify the origin of the negative charges. We were able to confirm that the local structures, which are the origin of the negative charges, are retained even after the removal of the potassium atoms. Finally, we propose guidelines for identifying the characteristic local structure.

The calculations were performed using the Vienna *Ab initio* Simulation Package (VASP), which is based on density functional theory.^{20–23} In the structural optimization, we stopped the calculations when the maximum force on each atom was less than 5.0×10^{-2} eV/Å. The nuclei and core electrons were simulated by pseudopotentials generated by the projector augmented-wave method.²⁴ The valence wave functions were expanded using the plane wave basis set, for which we found that a cutoff energy of 460 eV suffices. Twelve *k* points in a $2 \times 2 \times 3$ Monkhorst–Pack grid were sampled for the Brillouin zone integrations. We used a GGA-PBE-type exchange–correlation functional²⁵ for the molecular dynamics (MD) calculations and structural optimization. The Heyd, Scuseria, and Ernzerhof (HSE) exchange–correlation functional²⁶ was also used to obtain an accurate value for the energy of each structure. We set the fraction of the Fock exchange and the range-separation parameter in the HSE functional to be 0.51 and 0.20 Å⁻¹, respectively, which reproduces the bandgap of 9.0 eV for SiO₂. The volume of a supercell was fixed during all the calculations. We used a Bader charge analysis^{27–30} to investigate the charge states. The VESTA system was used to draw the atomic configurations.³¹

According to experimental reports, potassium-ion electrets are made using the steps illustrated in Fig. 1.^{7,32,33} First, a Si substrate is thermally oxidized by steam supplied through a KOH solution to obtain a-SiO₂ with potassium atoms. In this process, potassium and

hydrogen atoms are incorporated into the a-SiO₂. Thereafter, a high voltage (200 V) is applied while heating the a-SiO₂ with potassium atoms at 550 °C. During this process, the potassium ions move toward the cathode, and the low-potassium-density region becomes negatively charged. Finally, a negatively charged electret is fabricated by removing the cathode.

We created an a-SiO₂ structure with potassium atoms using the following steps. We prepared supercells of alpha quartz (144 atoms) and inserted one potassium and one hydrogen atom into each supercell. The insertion positions were randomly chosen and resulted in four initial structures. The density of a-SiO₂ was set to the experimentally obtained value of 2.2 g/cm³.³⁴ To obtain the amorphous structures, we performed melt–quench simulations using first-principles MD calculations. The temperature history used in these MD calculations was as follows. During the first 10 ps, the supercell was held at 5000 K to melt the structure, and it was then quenched to 0 K at a rate of 50 K/ps. The melt–quench technique has been extensively used in previous research to investigate a-SiO₂.^{35–39} It has been reported that a-SiO₂ can be formed at a cooling rate of 200 K/ps, and almost the same structures are obtained with a cooling rate of 100 K/ps.⁴⁰ Thus, the cooling rate we used is sufficiently slow to form a-SiO₂. After the MD calculations, we performed structural-optimization calculations for each structure obtained and examined the resulting characteristic structures. Thereafter, we removed the potassium atoms from the supercells and re-performed the MD calculations to anneal these models. The temperature history used in this second set of MD calculations was as follows. During the first 10 ps, the supercell was held at 1000 K, and it was then quenched to 0 K at a rate of 50 K/ps. After this, we again optimized each charged structure.

We begin with examinations of the structures obtained after the first MD calculations. The structure of a-SiO₂ with a potassium atom is shown in Fig. 2(a). We found that all four a-SiO₂/potassium-atom models had two characteristic structures: a fivefold-coordinated Si atom and a Si–Si bond structure. These special structures appear even though the potassium atom is not involved in their bonding. To investigate the effect of the potassium-atom insertion, we also created a simple a-SiO₂ structure using the same temperature history as the initial MD calculations. In this structure, all the Si atoms had four Si–O bonds and there was no characteristic local structure, as noted in previous reports.³⁶ Therefore, these local structures, a fivefold-coordinated Si atom and a Si–Si bond, are quite different from those of ordinary a-SiO₂ and are considered to be induced by the potassium atom.

Figure 2(b) shows the detailed structure around a potassium atom. The ionic valences obtained by a Bader charge analysis are also

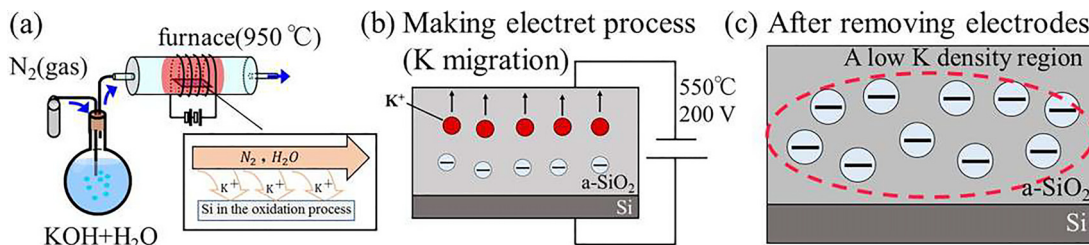


FIG. 1. Schematic illustration of fabrication of K-ion electrets. (a) Thermal oxidation, which incorporates K atoms into a-SiO₂. (b) Charge-storage mechanism of a K-ion electret. On applying a voltage while heating, the K ions move to the cathode. (c) The cathodes are removed. The low-K-density region is negatively charged.

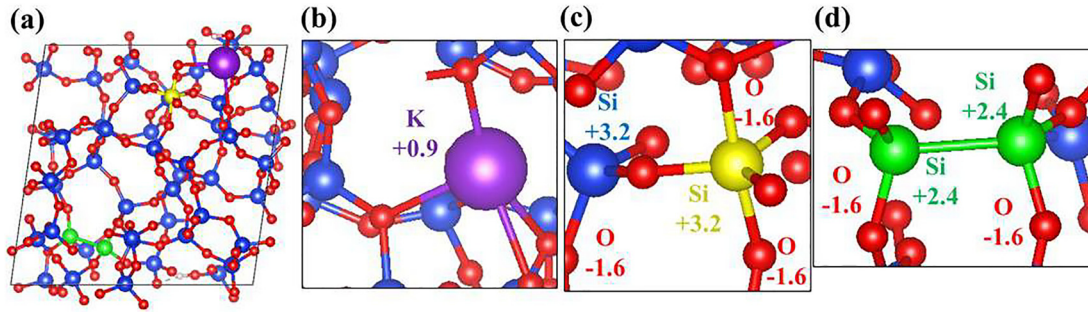


FIG. 2. (a) The a-SiO₂ structure obtained by the initial MD calculations. Some local structures are formed by inserting a K atom. Blue, red, and purple spheres denote Si, O, and K atoms, respectively. The characteristic local structures are shown in different colors. The yellow spheres are fivefold-coordinated Si atoms, which have five Si–O bonds. The green spheres are Si atoms with Si–Si bonds. (b) Structure around a potassium atom. The ionic valences obtained from a Bader charge analysis are also depicted. (c) Structure around a fivefold-coordinated Si atom. (d) Structure around a Si–Si bond. The ionic valences obtained from a Bader charge analysis are also depicted.

depicted. The interatomic distance between the potassium and oxygen atoms is about 3 Å, and the potassium and oxygen atoms do not form any bonds. From the Bader charge analysis, we found that the ionic valence of a potassium atom is +0.9 [Fig. 2(b)], indicating that it behaves as a positively charged ion. However, the ionic valence of the O atoms around the potassium atom is about –1.6, which is the same as the ionic valence in ordinary SiO₂. From the above discussion, it is considered that the potassium atom behaves as a mobile cation, and this result is in good agreement with experiments, in which the potassium atoms can move toward the cathode when a voltage is applied.⁷

Figure 2(c) shows the detailed structure around the fivefold-coordinated Si atom with five Si–O bonds. Previous studies have suggested that fivefold-coordinated Si atoms exist in K₂O–SiO₂ glasses,^{18,19} a-Si,^{41,42} and H-incorporated a-SiO₂.⁴³ Since a Si atom usually has four bonds, the presence of a fivefold-coordinated Si atom with five Si–O bonds is quite characteristic. We call this structure an SiO₅ structure. The usual fourfold-coordinated structure is an SiO₄ structure. The ionic valences of a Si atom and five O atoms in an SiO₅ structure are about +3.2 and –1.6, which are almost the same as the values in an SiO₄ structure. Since each O atom forms two Si–O bonds, the ionic valence of an O atom per Si atom is –0.8. Accordingly, the total ionic valence of an SiO₄ structure is found to be 0.0, indicating that SiO₄ structures are electrically neutral. However, since an SiO₅ structure consists of a Si atom with an ionic valence of +3.2 and five oxygen atoms, each with an ionic valence of –0.8, the total ionic valence of an SiO₅ structure is –0.8. Thus, we find that the SiO₅ structure is negatively charged in a-SiO₂ with a potassium atom.

Figure 2(d) shows the detailed structure around the Si–Si bond structure. The ionic valences of Si and O atoms are +2.4 and –1.6, respectively. This structure consists of two Si atoms with an ionic valence of +2.4 and six O atoms, each with an ionic valence of –0.8. The total ionic valence of these atoms is, therefore, 0.0. This indicates that this Si–Si bond structure is electrically neutral. As discussed above, charge transfer from the potassium atom to the SiO₅ structure occurs, resulting in the presence of K⁺ ions and negatively charged SiO₅ structures.

We now discuss the atomic and electronic structures of a-SiO₂ after potassium-atom removal. Experimentally, it has been reported that potassium-ion electrets are negatively charged after removal of their potassium atoms. However, it is well known that a stable charged

state sensitively depends on the position of the Fermi level. To consider the relative stability of the neutral state and the negatively and positively charged states, we calculated the formation energy of the charged system (E_{form}) using^{44,45}

$$E_{\text{form}} = (E_{\text{defect}}(q) + E_{\text{quartz}}(0)) - (E_{\text{defect}}(0) + E_{\text{quartz}}(q)) + \frac{3q^2}{10\epsilon r_0} + \begin{cases} qE_{\text{F}} & (q \geq 0), \\ q(E_{\text{F}} - E_{\text{gap}}) & (q < 0), \end{cases} \quad (1)$$

where E_{defect} is the energy of a crystal with a defect, E_{quartz} is the energy of quartz SiO₂, E_{gap} is the bandgap, ϵ is the dielectric constant, r_0 is the radius of a sphere with the same volume as a unit cell, q is the charge state, and E_{F} is the Fermi level of the system measured from the top of the valence band.

Figure 3 shows the formation energy of each charged state, and it can be seen that positively or negatively charged states are always more stable than the neutral state. Hence, we focus on the negatively and positively charged states. For the negatively charged state, the SiO₅ structure remains in a-SiO₂ even after removal of the potassium atom from the supercell. We performed a Bader charge analysis for these

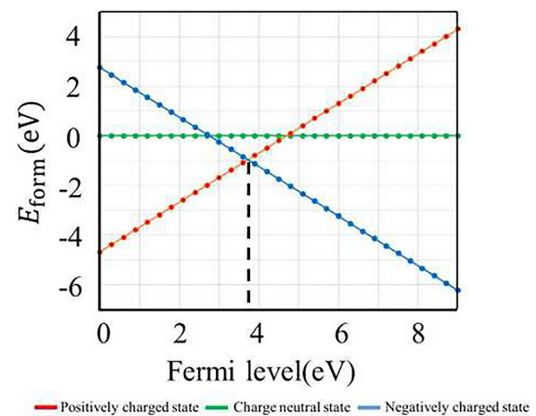


FIG. 3. Formation energy diagram after removal of the K⁺ ion. The negatively charged state becomes stable when the Fermi level is higher than 3.7 eV. We set the energy of the neutral charged state to 0.

local structures and found that the SiO_5 structure is negatively charged and that the Si–Si bond structure is electrically neutral. For the positively charged state, the Si–Si bond is broken, and two Si dangling bonds appear, although the fivefold-coordinated SiO_5 structure is preserved. The formation of Si dangling bonds upon hole injection is consistent with a previous report.⁴⁶ From the Bader charge analysis, it was found that the fivefold-coordinated SiO_5 structure still retains an electron and remains negatively charged even after electron removal. Next, we looked at the Si dangling bonds in the positively charged state. From the Bader charge analysis, we found that the ionic valence of threefold-coordinated Si is +3.1, which is almost the same as that of the fourfold-coordinated SiO_4 structure. Because Si atoms with a dangling bond have three Si–O bonds, the Si-dangling-bond structure is positively charged. Accordingly, we can conclude that the system is positively charged due to the two positively charged Si dangling bonds.

More importantly, it was found that the intersection between the positively and negatively charged states is located at 3.7 eV. This result means that the stable charge state of a- SiO_2 completely reverses between positively and negatively charged states at a threshold of 3.7 eV. To obtain stable negatively charged potassium-ion electrets, the system Fermi level should be greater than 3.7 eV in the process conditions. In other words, lowering the Fermi level induces the appearance of positively charged Si-dangling-bond structures.

We now discuss the Fermi level condition during the experimental conditions. In the fabrication process of an electret,⁷ there is a Si substrate below the potassium-ion electret itself [Fig. 1(b)]. Thus, it is estimated that the position of the Fermi level in the SiO_2 is determined by the Fermi level position of the Si substrate, and the band offset at the Si/ SiO_2 interface has already been reported by a theoretical study (Fig. 4).⁴⁷ Since the Fermi level of Si is within the bandgap, the Fermi level at the Si/ SiO_2 interface is located between 4.4 eV and 5.5 eV above the top of the valence band of SiO_2 . In this region, the negatively charged state becomes the most stable configuration (Fig. 4). Consequently, experimentally obtained potassium-ion electrets with Si substrates spontaneously form SiO_5 structures and store a negative charge. It is expected that this negative charge can be almost permanently retained due to the high strength of Si–O bonds and that potassium-ion electrets should, therefore, enable the realization of high-reliability vibration-powered generators. Moreover, the higher the Fermi level, the more stable the negatively charged state. Therefore, we can conclude that a potassium-ion electret produced from an n-type Si substrate will be more reliable than the one

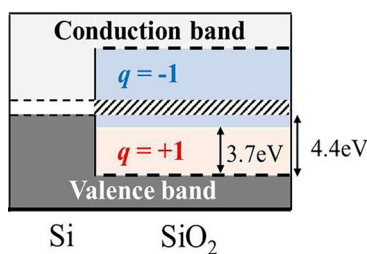


FIG. 4. Schematic band diagram of the Si/ SiO_2 interface with the stable charged state. The Fermi level at the Si/ SiO_2 interface is dominated by the Fermi level of Si. The striped area is the Fermi level of the system. The negatively charged state is always stable when we use Si substrates.

produced from a p-type Si substrate. Moreover, using an n-type Si substrate is also promising because its Fermi level is located higher than that of an n-type Si substrate.

Finally, we consider guidelines for identifying the fivefold-coordinated SiO_5 structure. Raman spectroscopy is effective for observing local structures^{48,49} because it measures the eigenfrequency of a crystal as a Raman shift. Thus, we calculated the eigenfrequencies of the fivefold-coordinated SiO_5 structure to be about 1000 cm^{-1} and 400 cm^{-1} . We also calculated the Raman scattering activity⁵⁰ for each vibration mode and determined that these two vibration modes can be observed by Raman spectroscopy. We next calculated the eigenfrequency of the fourfold-coordinated SiO_4 structure to be about 400 cm^{-1} . Thus, the 1000 cm^{-1} eigenfrequency of a fivefold-coordinated SiO_5 structure is far from the eigenfrequency of the usual fourfold-coordinated SiO_4 structures and can be used to identify the SiO_5 structure. Therefore, fivefold-coordinated SiO_5 structures can be identified by a Raman peak at 1000 cm^{-1} .

In summary, we have proposed a mechanism for the storage of negative charge by potassium-ion electrets based on first-principles calculations. In this study, we modeled the manufacturing of potassium-ion electrets by first-principles MD calculations and investigated the structures and the charged states of a- SiO_2 with and without a potassium atom. We found that characteristic local structures, such as the fivefold-coordinated SiO_5 structure, appear in a- SiO_2 with a potassium atom. These local structures were produced by inserting a potassium atom. The potassium atom is positively charged, whereas the fivefold-coordinated SiO_5 structure is negatively charged. Next, we estimated the stability of the charge state after removal of the potassium atom by comparing the formation energies of each charged state as functions of the Fermi level. The negatively charged state was found to be the most stable in the experimental conditions, and the negatively charged SiO_5 structure is retained. Therefore, we conclude that the fivefold-coordinated SiO_5 structure is the physical origin of the robust storage of negative charge in potassium-ion electrets. Since the Si–O bond is extraordinarily strong, it is expected that the negative charge will be almost permanently retained. Therefore, potassium-ion electrets can be used to fabricate high-reliability vibration-powered generators. This result is in good agreement with the experimental results for a negatively charged electret. Finally, we propose that fivefold-coordinated SiO_5 structures can be identified experimentally because they will have a Raman peak at 1000 cm^{-1} .

This work was supported by the Ministry of Education, Culture, Sports, Science, and Technology, Japan, under the research project “Promoting Research on the Supercomputer Fugaku” and by the Japan Science and Technology Agency for Core Research for Evolutional Science and Technology (Grant Nos. JPMJCR15Q4 and JPMJCR19Q2).

DATA AVAILABILITY

The data that support the findings of this study are available from the corresponding author upon reasonable request.

REFERENCES

- ¹Y. Suzuki, *J. Jpn. Soc. Appl. Electromagn. Mech.* **22**, 339 (2014).
- ²S. Roundy, P. K. Wright, and J. Rabaey, *Comput. Commun.* **26**, 1131 (2003).
- ³J. A. Paradiso and T. Starner, *IEEE Pervasive Comput.* **4**, 18 (2005).
- ⁴R. J. M. Vullers, R. van Schaijk, H. J. Visser, J. Penders, and C. Van Hoof, *IEEE Solid-State Circuits Mag.* **2**, 29 (2010).
- ⁵S. Kaminaga, *Sens. Mater.* **30**, 723 (2018).

- ⁶H. Toshiyoshi, S. Ju, H. Honma, C.-H. Ji, and H. Fujita, *Sci. Technol. Adv. Mater.* **20**, 124 (2019).
- ⁷G. Hashiguchi, D. Nakasone, T. Sugiyama, M. Ataka, and H. Toshiyoshi, *AIP Adv.* **6**, 035004 (2016).
- ⁸M. Suzuki, H. Ashizawa, Y. Fujita, H. Mitsuya, T. Sugiyama, M. Ataka, H. Toshiyoshi, and G. Hashiguchi, *J. Microelectromech. Syst.* **25**, 652 (2016).
- ⁹H. Koga, H. Mitsuya, H. Honma, H. Fujita, H. Toshiyoshi, and G. Hashiguchi, *Micromachines* **8**, 293 (2017).
- ¹⁰Y. Tohyama, H. Honma, B. Durand, T. Sugiyama, G. Hashiguchi, and H. Toshiyoshi, *Sens. Mater.* **31**, 2779–2802 (2019).
- ¹¹H. Toshiyoshi, H. Honma, H. Mitsuya, and G. Hashiguchi, *Vac. Surf. Sci.* **63**, 223 (2020).
- ¹²C. Sano, M. Ataka, G. Hashiguchi, and H. Toshiyoshi, *Micromachines* **11**, 267 (2020).
- ¹³K. Misawa, T. Sugiyama, G. Hashiguchi, and H. Toshiyoshi, *Jpn. J. Appl. Phys., Part 1* **54**, 067201 (2015).
- ¹⁴C. Haug and A. N. Cormack, *J. Chem. Phys.* **95**, 3634 (1991).
- ¹⁵S. Balasubramanian and K. J. Rao, *J. Phys. Chem.* **98**, 10871 (1994).
- ¹⁶S. Sen and R. E. Youngman, *J. Non-Cryst. Solids* **331**, 100 (2003).
- ¹⁷R. Sawyer, H. W. Nesbitt, and R. A. Secco, *J. Non-Cryst. Solids* **358**, 290 (2012).
- ¹⁸J. F. Stebbins, *Nature* **351**, 638 (1991).
- ¹⁹J. F. Stebbins and P. McMillan, *J. Non-Cryst. Solids* **160**, 116 (1993).
- ²⁰G. Kresse and J. Hafner, *Phys. Rev. B* **47**, 558 (1993).
- ²¹G. Kresse and J. Hafner, *Phys. Rev. B* **49**, 14251 (1994).
- ²²G. Kresse and J. Furthmüller, *Phys. Rev. B* **54**, 11169 (1996).
- ²³G. Kresse and D. Joubert, *Phys. Rev. B* **59**, 1758 (1999).
- ²⁴P. E. Blochl, *Phys. Rev. B* **50**, 17953 (1994).
- ²⁵J. P. Perdew, K. Burke, and M. Ernzerhof, *Phys. Rev. Lett.* **77**, 3865 (1996).
- ²⁶J. Heyd, G. E. Scuseria, and M. Ernzerhof, *J. Chem. Phys.* **118**, 8207 (2003).
- ²⁷W. Tang, E. Sanville, and G. Henkelman, *J. Phys.: Condens. Matter* **21**, 084204 (2009).
- ²⁸E. Sanville, S. D. Kenny, R. Smith, and G. Henkelman, *J. Comput. Chem.* **28**, 899 (2007).
- ²⁹G. Henkelman, A. Arnaldsson, and H. Jónsson, *Comput. Mater. Sci.* **36**, 354 (2006).
- ³⁰M. Yu and D. R. Trinkle, *J. Chem. Phys.* **134**, 064111 (2011).
- ³¹K. Momma and F. Izumi, *J. Appl. Crystallogr.* **44**, 1272 (2011).
- ³²T. Sugiyama, M. Aoyama, Y. Shibata, M. Suzuki, T. Konno, M. Ataka, H. Fujita, and G. Hashiguchi, *Appl. Phys. Express* **4**, 114103 (2011).
- ³³Y. Shibata, T. Sugiyama, H. Mimura, and G. Hashiguchi, *J. Microelectromech. Syst.* **24**, 1052 (2015).
- ³⁴N. L. Anderson, R. P. Vedula, P. A. Schultz, R. M. Van Ginhoven, and A. Strachan, *Phys. Rev. Lett.* **106**, 206402 (2011).
- ³⁵K. Vollmayr, W. Kob, and K. Binder, *Phys. Rev. B* **54**, 15808 (1996).
- ³⁶S. von Alffhan, A. Kuronen, and K. Kaski, *Phys. Rev. B* **68**, 073203 (2003).
- ³⁷R. M. Van Ginhoven, H. Jónsson, and L. R. Corrales, *Phys. Rev. B* **71**, 024208 (2005).
- ³⁸M. Kim, K. H. Khoo, and J. R. Chelikowsky, *Phys. Rev. B* **86**, 054104 (2012).
- ³⁹J. M. D. Lane, *Phys. Rev. E* **92**, 012320 (2015).
- ⁴⁰K. Chokawa, T. Narita, D. Kikuta, K. Shiozaki, T. Kachi, A. Oshiyama, and K. Shiraishi, *Phys. Rev. Appl.* **14**, 014034 (2020).
- ⁴¹S. T. Pantelides, *Phys. Rev. Lett.* **58**, 1344 (1987).
- ⁴²N. Ishii and T. Shimizu, *Jpn. J. Appl. Phys., Part 2* **27**, L1800 (1988).
- ⁴³J. Godet and A. Pasquarello, *Microelectron. Eng.* **80**, 288 (2005).
- ⁴⁴P. E. Blöchl, *Phys. Rev. B* **62**, 6158 (2000).
- ⁴⁵K. Yamaguchi, A. Otake, K. Kamiya, Y. Shigetani, and K. Shiraishi, *Jpn. J. Appl. Phys., Part 1* **50**, 04DD05 (2011).
- ⁴⁶A. Oshiyama, *Jpn. J. Appl. Phys., Part 2* **37**, L232 (1998).
- ⁴⁷J. Robertson, *J. Vac. Sci. Technol., B* **18**, 1785 (2000).
- ⁴⁸M. Cardona and G. Güntherodt, *Light Scattering in Solids* (Springer, Berlin, 1982), Vol. II.
- ⁴⁹P. Brüesch, *Phonons: Theory and Experiments* (Springer, Berlin, 1986), Vol. II.
- ⁵⁰D. Porezag and M. R. Pederson, *Phys. Rev. B* **54**, 7830 (1996).